Journal of Physiology - Paris xxx (2009) xxx–xxx

Contents lists available at ScienceDirect

Journal of Physiology - Paris

journal homepage: www.elsevier.com/locate/jphysparis

Voltage-sensitive dye imaging: Technique review and models

S. Chemla [a,*], F. Chavane [b]

[a] NeuroMathComp Team, INRIA Sophia-Antipolis, 2004 route des Lucioles, 06902 Sophia-Antipolis, France
[b] Institut de Neurosciences Cognitives de la Mediterranee, CNRS, Aix-Marseille University, UMR6193, 31 Chemin Joseph Aiguier, 13402 Marseille, France

ARTICLE INFO

Article history:
Available online xxxx

Keywords:
Biophysical model
Cortical column
Optical imaging
Mesoscopic scale
Voltage-sensitive dyes

ABSTRACT

In this review, we present the voltage-sensitive dye imaging (VSDI) method. The possibility offered for *in vivo* (and *in vitro*) brain imaging is unprecedented in terms of spatial and temporal resolution. However, the unresolved multi-component origin of the optical signal encourages us to perform a detailed analysis of the method limitation and the existing models. We propose a biophysical model at a mesoscopic scale in order to understand and interpret this signal.

Contents

* Corresponding author.
E-mail address: sandrine.chemla@sophia.inria.fr (S. Chemla).

0928-4257/$ - see front matter © 2009 Elsevier Ltd. All rights reserved.
doi:10.1016/j.jphysparis.2009.11.009

Please cite this article in press as: Chemla, S., Chavane, F. Voltage-sensitive dye imaging: Technique review and models. J. Physiol. (2009), doi:10.1016/j.jphysparis.2009.11.009

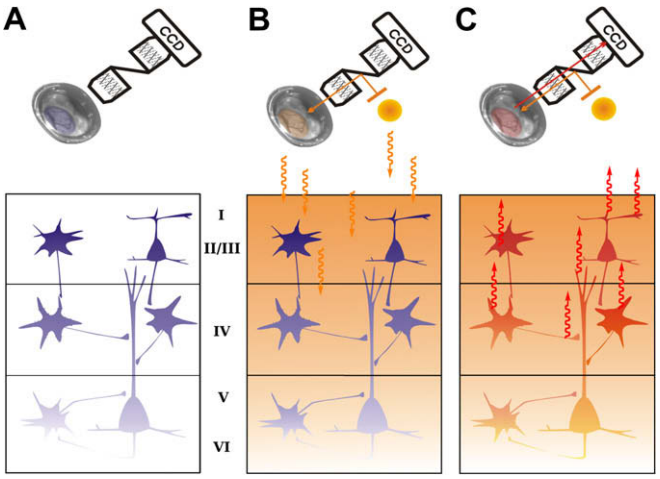

Fig. 1. VSDI principle in three steps. The imaging chamber allows a direct access of the primary visual cortex V1 represented as a patch of cortex with its six layers. (A) The dye, applied on the surface of the cortex, penetrates through the cortical layers of V1. (B) All neuronal and non-neuronal cells are now stained with the dye and when the cortex is illuminated, the dye molecules act as molecular transducers that transform changes in membrane potential into optical signals. (C) The fluorescent signal (red arrow) is recorded by a CCD camera.

1. Introduction

Optical imaging comes within the scope of new imaging techniques that allow us to visualize the functioning brain at both high spatial and temporal resolutions. Specifically, there are two techniques mostly used *in vivo* (see Grinvald et al. (1999) for a detailed review); the first is based on intrinsic signals, and the second is based on voltage-sensitive dyes (VSDs). In this review, we focus on the second technique, aiming at better understand the origin of the optical signal. Extensive reviews of VSDI have been published elsewhere (e.g. Grinvald et al., 2004; Roland, 2002). Although the underlying mechanism of this optical method is nowadays well understood, the recorded signal remains very complex and it seems difficult to isolate the contributions from its different components. This review suggests modeling as the appropriate solution. Few models of the VSD signal exist that help to understand the optical signal in terms of functional organization and dynamics of a population neural network. A closer interaction between VSDI experimentalists and modelers is desirable.

In the first part of this review, we give a general introduction to VSDI, followed by examples of applications to brain imaging. We compare *in vitro* and *in vivo* recordings obtained with VSDI in several animal studies. In a second part, we make the underlying limitations of this method explicit: what does the VSD signal measure? A question that is not completely answered in the literature. Finally, this review shows the benefit of brain activity modeling for optical signal analysis. Models of VSDI measures are reported. We both address what has already been done and what will be interesting to do in order to interpret the origins of the optical imaging signal.

2. VSDI for beginners

2.1. General principle

VSDI offers the possibility to visualize, in real time, the cortical activity of large neuronal populations with high spatial resolution (down to 20–50 μm) and high temporal resolution (down to the millisecond). With such resolutions, VSDI appears to be the best technique to study the dynamics of cortical processing at neuronal population level.

This invasive technique is also called "extrinsic optical imaging" because of the use of voltage-sensitive dyes (Cohen et al., 1974; Ross et al., 1977; Waggoner and Grinvald, 1977; Gupta et al., 1981). After opening the skull and the dura mater of the animal, the dye molecules are applied on the surface of the cortex (Fig. 1A). They bind to the external surface of the membranes of all cells without interrupting their normal function and act as molecular transducers that transform changes in membrane potential into optical signals. More precisely, once excited with the appropriate wavelength (Fig. 1B), VSDs emit instantaneously an amount of fluorescent light that is function of changes in membrane potential, thus allowing for an excellent temporal resolution for neuronal activity imaging (Fig. 1C). The fluorescent signal is proportional to the membrane area of all stained elements under each measuring pixel.

"All elements" means all neuronal cells present in the cortex but also all non-neuronal cells, like glial cells (see Section 3.1 for more details). Moreover, neuronal cells include excitatory cells and inhibitory cells, whose morphology and intrinsic properties are quite different (see Salin and Bullier (1995) for a review on the different type of neurons and connections in the visual cortex). Furthermore, each cell has various compartments, including dendrites, somata and axons. The measured signal thus combine all these components, which are all likely to be stained in the same manner. The dye concentration is only depending on the depth of the cortex.

The fluorescent signal is then recorded by the camera of the optical video imaging device and displayed as dynamic sequences on computer (see Fig. 1). The submillisecond temporal resolution is reached by using ultra sensitive charge-coupled device (CCD) camera, whereas the spatial resolution is limited by optical scattering of the emitted fluorescence (Orbach and Cohen, 1983).

2.2. Optical imaging of neuronal population activity

2.2.1. General history

The earliest optical recordings were made, at the single neuron level, both from cultured cells (Tasaki et al., 1968) and from various invertebrate preparations like ganglia of the leech (Salzberg et al., 1973), or the giant axon of the squid (Davila et al., 1973). For all other VSDI experiments, the VSD signal has a neuronal population resolution.

The VSDI method has then been used *in vitro* on brain slices, mainly in rodent and ferret. It allowed to optically record from the hippocampus (Grinvald et al., 1982), the visual cortex (Bolz et al., 1992; Albowitz and Kuhnt, 1993; Nelson and Katz, 1995; Yuste et al., 1997; Contreras and Llinas, 2001; Tucker and Katz, 2003a; Tucker and Katz, 2003b), the somatosensory cortex (Yuste et al., 1997; Antic et al., 1999; Contreras and Llinas, 2001; Petersen et al., 2001; Jin et al., 2002; Laaris and Keller, 2002; Berger et al., 2007) and from the auditory cortex (Jin et al., 2002; Kubota et al., 2006).

The salamander, largely used *in vitro* (Orbach and Cohen, 1983; Cinelli and Salzberg, 1992), was the first species also used *in vivo* for studying the olfactory system using VSDI (Orbach and Cohen, 1983), followed by the frog for the visual system (Grinvald et al., 1984), and the rodent for the somatosensory system. Indeed, initial *in vivo* studies of the somatosensory cortex have been made in anesthetized rodents, taking advantage of the thinness of the cortical dura (Orbach et al., 1985). More recently, VSDI in freely moving mice has also been performed with success (Ferezou et al., 2006).

Rodent and ferret were also used for studying the visual cortex *in vivo* (Roland et al., 2006; Lippert et al., 2007; Xu et al., 2007;

Please cite this article in press as: Chemla, S., Chavane, F. Voltage-sensitive dye imaging: Technique review and models. J. Physiol. (2009), doi:10.1016/j.jphysparis.2009.11.009

Ahmed et al., 2008). However, the main VSDI experiments on visual modality were conducted on two other mammalian species: cat and monkey (Grinvald et al., 1994; Arieli et al., 1995; Sterkin et al., 1998; Shoham et al., 1999; Sharon and Grinvald, 2002; Slovin et al., 2002; Seidemann et al., 2002; Jancke et al., 2004; Sharon et al., 2007; Benucci et al., 2007; Reynaud et al., 2007; Yang et al., 2007). Experiments on anesthetized cats are very attractive for mapping and studying the primary visual cortex, whereas monkey experiments also associate behavioral measures.

2.2.2. High spatial resolution for brain mapping

One domain of application of the VSDI, as other brain functional imaging, is brain mapping. Indeed, VSDI allows to build high-resolution functional maps, such as orientation or ocular-dominance maps (Shoham et al., 1999; Grinvald et al., 1999; Slovin et al., 2002; Sharon and Grinvald, 2002), as also obtained with optical imaging based on intrinsic signals (ISI) (Blasdel and Salama, 1986; Ts'o et al., 1990; Grinvald et al., 1991; Bonhoeffer and Grinvald, 1991; Hubener et al., 1997; Rubin and Katz, 1999). Comparison between the two imaging techniques (Shoham et al., 1999; Grinvald et al., 1999; Slovin et al., 2002) confirms the high spatial resolution of VSDI methodology for mapping the functional architecture of the visual cortex. However, although it is possible to do such brain mapping using VSDI, it does not take advantage of the possibility to inspect neuronal activation dynamics.

2.2.3. High temporal resolution unveils the dynamics of cortical processing

The main benefit of the VSDI technique is the possibility for neuroscientists to go further electrophysiological studies and low resolution (either temporal or spatial) imaging techniques, since visualizing in real time with high spatial resolution large populations of neurons, while supplying information about cortical networks temporal dynamics. Many neuroscientists are motivated to investigate how a sensory stimulus is represented dynamically on the cortical surface in space and time (Grinvald et al., 1984; Grinvald et al., 1994; Arieli et al., 1996; Petersen et al., 2003; Civillico and Contreras, 2006). More precisely, the spatiotemporal dynamics of the response to simple stimuli, e.g. local drifting-oriented gratings or single whisker stimulation, have been visualized using VSDI on *in vivo* preparations (Cat: Sharon et al., 2007; Rodent: Petersen et al., 2003). Complex stimuli, e.g. the line motion or apparent motion illusions, have also been achieved using VSDI in the visual cortex of cats (Jancke et al., 2004) or ferrets (Ahmed et al., 2008), revealing fundamental principles of cortical processing *in vivo*. Nowadays, rapid and precise dynamic functional maps can even be obtained on behaving animals, as shown by Seidemann et al. (2002), Slovin et al. (2002) and Yang et al. (2007) on behaving monkeys, or by Ferezou et al. (2006) in freely moving mice.

There questions are conceivable thanks to the persistent development of novel dyes (Shoham et al., 1999; Grinvald et al., 2004; Kee et al., 2009). Indeed, the developed dyes allowed to monitor in real time neuronal activation both in *in vivo* and *in vitro* preparations (Arieli et al., 1996; Grinvald et al., 1999; Petersen et al., 2001; Petersen et al., 2003).

2.2.4. Functional connectivity reveals its dynamics

Combining the spatial and temporal advantages, an other direct application of VSDI is the possibility to study the functional con-

Table 1
Non-exhaustive list of publications related to VSDI, classified by experimental conditions (either *in vitro* or *in vivo*) and by species.

Conditions	Species	Related publications	Structure	Dye	λ_{exc} (nm)
In vitro (invertebrate preparations, cultured cells or brain slices)	Invertebrate (squid, skate, snail, leech)	Tasaki et al. (1968), Davila et al. (1973), Salzberg et al. (1973), Woolum and Strumwasser (1978), Gupta et al. (1981), Konnerth et al. (1987), Cinelli and Salzberg (1990), Antic and Zecevic (1995), and Zochowski et al. (2000)	Giant neurons	Styryl JPW1114 optimized for intracellular applications	540
			Axons	JPW1114 (fluorescence)	520
			Cerebellar parallel fibres	Pyrazo-oxonol RH482, RH155 (absorption)	
	Goldfish	Manis and Freeman (1988)	Optic tectum	Styryl RH414 (fluorescence)	540
	Salamander	Orbach and Cohen (1983) and Cinelli and Salzberg (1992)	Olfactory bulb	Merocyanine XVII optimized for absorption measurements (Ross et al., 1977; Gupta et al., 1981), RH414, RH155	
	Rodent	Grinvald et al. (1982), Bolz et al. (1992), Albowitz and Kuhnt (1993), Yuste et al. (1997), Antic et al. (1999), Petersen et al. (2001), Contreras and Llinas (2001), Laaris and Keller (2002), Jin et al. (2002), Kubota et al. (2006), Berger et al. (2007), Carlson and Coulter (2008), and Kee et al. (2009)	Visual cortex	Fluorochrome Di-4-ANEPPS, RH414, Styryl RH795 (fluorescence)	500, 540
			Barrel cortex	JPW2038, RH155, RH482, NK3630, JPW1114, RH414, RH795	
			Auditory cortex	RH795 for fluorescence, Oxonol NK3630 for absorption	520, 705
			hippocampus	WW401	520
	Ferret	Nelson and Katz (1995) and Tucker and Katz (2003a,b)	Visual cortex	RH461 (fluorescence)	590
In vivo (anesthetized or awake)	Frog	Grinvald et al. (1984)	Visual cortex	Styryl RH414	520
	Salamander	Orbach and Cohen (1983) and Kauer (1988)	Olfactory bulb	Styryl RH160 and RH414 optimized for fluorescence measurements (Grinvald et al., 1982)	510, 540
	Rodent	Orbach et al. (1985), Orbach and Van Essen (1993), Petersen et al. (2003), Derdikman et al. (2003), Civillico and Contreras (2006), Ferezou et al. (2006), Berger et al. (2007), Lippert et al. (2007), Xu et al. (2007), and Brown et al. (2009)	Barrel cortex	RH795, Oxonol RH1691, RH1692 and RH1838 optimized for in vivo fluorescent measurements (Shoham et al., 1999; Spors et al., 2002)	540, 630
			Visual cortex	RH1691, RH1838	630
	Ferret	Roland et al. (2006) and Ahmed et al. (2008)	Visual cortex	RH795, RH1691	530, 630
	Cat	Arieli et al. (1995), Sterkin et al. (1998), Shoham et al. (1999), Sharon and Grinvald (2002), Jancke et al. (2004), Sharon et al. (2007), and Benucci et al. (2007)	Visual cortex (area 17/18)	RH795, RH1692	530-40, 630
	Monkey	Grinvald et al. (1994), Shoham et al. (1999), Slovin et al. (2002), Seidemann et al. (2002), Reynaud et al. (2007), and Yang et al. (2007)	Visual cortex (V1/V2)	RH1691, RH1692, RH1838	630
			FEF	RH1691	630

Please cite this article in press as: Chemla, S., Chavane, F. Voltage-sensitive dye imaging: Technique review and models. J. Physiol. (2009), doi:10.1016/j.jphysparis.2009.11.009

nectivity of neuronal populations. Yuste et al. (1997) for example, investigated the connectivity diagram of rat visual cortex using VSDI. Vertical and horizontal connections have been detected. More generally, intracortical and intercortical interactions, occurring during sensory processing (especially visual), have been largely explored using VSDI, either *in vitro* or *in vivo*: Mapping functional connections using VSDI, has been done *in vitro* in the rat visual cortex (Bolz et al., 1992; Carlson and Coulter, 2008), in the guinea pig visual cortex (Albowitz and Kuhnt, 1993) and in the ferret visual cortex (Nelson and Katz, 1995; Tucker and Katz, 2003a; Tucker and Katz, 2003b), providing not only functional, but also anatomical and physiological information on the local network. For example, Tucker and Katz (2003a) investigated with VSDI how neurons in layer 2/3 of ferret visual cortex integrate convergent horizontal connections.

Orbach and Van Essen (1993) used VSDI in the visual system of the rat *in vivo* to map striate and extrastriate pathways. Feedforward propagating waves from V1 to other cortical areas, and feedback waves from V2 to V1 have been recently reported by Xu et al. (2007), thanks to VSDI. In addition, feedback depolarization waves (from areas 21 and 19 toward areas 18 and 17) were extensively studied by Roland et al. (2006) in ferrets after staining the visual cortex with VSD.

2.3. Conclusion

By adding a new dimension to existing brain functional imaging techniques, VSDI directly reports the spatiotemporal dynamics of neuronal populations activity. Many VSDI studies have then been conducted in order to investigate the spatiotemporal patterns of activity occurring in different parts of the CNS, *in vitro* or *in vivo*, on several preparations or animal species. The Table 1 lists most articles presenting experimental results using VSDI techniques. The publications are first classified by the condition of the experiment, either *in* vitro or *in vivo*, and then by the experimental preparations or animal species. Additional information about dyes is available in the last columns (see Ebner and Chen (1995) for a compilation of the commonly used dyes and their properties).

3. The multi-component origin of the optical signal

3.1. About the contribution from glial cells

In general, glial cells have been neglected by neuroscientists for a long time, especially because unlike neurons, they do not carry action potentials. However, glial cells have important functions (see Cameron and Rakic (1991) for a review) and they may contribute to the VSD signal.

Glial cells are known as the "supporting cells" of the CNS and are estimated to outnumber neurons by as much as 50–1. However, their role in information representation or processing remains unresolved. Indeed, *in vitro* studies have shown increasing evidence for an active role of astrocytes in brain function. However, little is known about the behavior of astrocytes *in vivo*.

When interpreting the VSD signal, we face two conflicting viewpoints. Konnerth and Orkand (1986), Lev-Ram and Grinvald (1986), Konnerth et al. (1987), Konnerth et al. (1988) and Manis and Freeman (1988) showed that the optical signal has two components: a "fast" followed by a "slow" signal. The latter has been revealed by doing successive staining with different dyes (e.g. RH482 and RH155), since each of them may preferentially stain different neuronal membranes. The authors then present evidence that this slow signal has a glial origin.

However, Kelly and Van Essen (1974) showed that the glial responses are weak (depolarizations of only 1–7 mV in response to visual stimuli) and have a time scale of seconds. Recent paper of Schummers et al. (2008) confirms that the astrocyte response is delayed 3–4 s from stimulus onset, which is a very slow temporal response compared to neuron response. Generally, in VSDI, only the first 1000 ms are considered, since intrinsic activity may affect the signal after this time.

We understand here that the controversy about glial contribution is directly link to the used dye (Ebner and Chen, 1995), and the time course of the optical signal generated. Thus, glial activity is very unlikely to participate significantly to the VSD signal (when considering recent fast dyes), since the amplitude of glial response is weak and its time course is very slow.

3.2. About the contribution from excitatory versus inhibitory cells

In the neocortex, neurons (despite their morphologic diversity) can be functionally classified in two groups: excitatory neurons, which represent about 80% of the cortical cells, and inhibitory neurons which represent about 20% of cortical cells (Douglas and Martin, 1990). Thus, it is tempting to say that the VSD signal mainly reflects the activity of excitatory neurons (Grinvald et al., 1999).

However, the VSD signal is proportional to changes in membrane potential. Thus, both excitatory and inhibitory neurons contribute positively to the VSD signal and it is hard to teaze apart contributions from excitatory or inhibitory cells. An additional level of complexity arises from the fact that inhibition operates generally in a shunting "silent" mode (Borg-Graham et al., 1998). In this mode, inhibition suppresses synaptic excitation without hyperpolarizing the membrane potential.

To conclude, the contribution of inhibitory cells to the VSD signal is unclear and would obviously benefit from modeling studies.

3.3. About the contribution from the various compartments

Neurons can be also decomposed into their main various compartments, whose surface and electrical activity are different (see Fig. 2, green part):

(a) The soma, whose electrical activity can be either synaptic (SP for synaptic potential) or spiking (AP for action potential).
(b) The dendrites, that integrate presynaptic AP information from others cells. The electrical activity is mainly synaptic, however, back-propagating AP could be recorded in the dendrites (see Waters et al. (2005) for a review). Dendritic surface area of mammalian neurons have been estimated by Sholl (1955a), Aitken (1955), and Young (1958) to be 10–12 times larger than cell bodies surface area, and to represents 90% of the total neuronal cell membrane (Eberwine, 2001).
(c) The axon, which carries spiking signals from the soma to the axon terminal. Spiking activity can be recorded on this part of neuron. In contrast with dendrites, the surface area of axons represents 1% of the total neuronal cell surface (Eberwine, 2001).

In the literature, regarding the difference in membrane areas of the various neuronal components and the nature of the signal, it is commonly accepted that the optical signal, in a given pixel, mostly originates from the dendrites of cortical cells, and therefore, mainly reflects dendritic post-synaptic activity (Orbach et al., 1985; Grinvald et al., 2004). Extensive comparisons between intracellular recordings from a single neuron and VSDI also showed that the optical signal correlates closely with synaptic membrane potential changes (Petersen et al., 2003; Contreras and Llinas, 2001). However, no real quantitative analysis has been performed to date

Please cite this article in press as: Chemla, S., Chavane, F. Voltage-sensitive dye imaging: Technique review and models. J. Physiol. (2009), doi:10.1016/j.jphysparis.2009.11.009

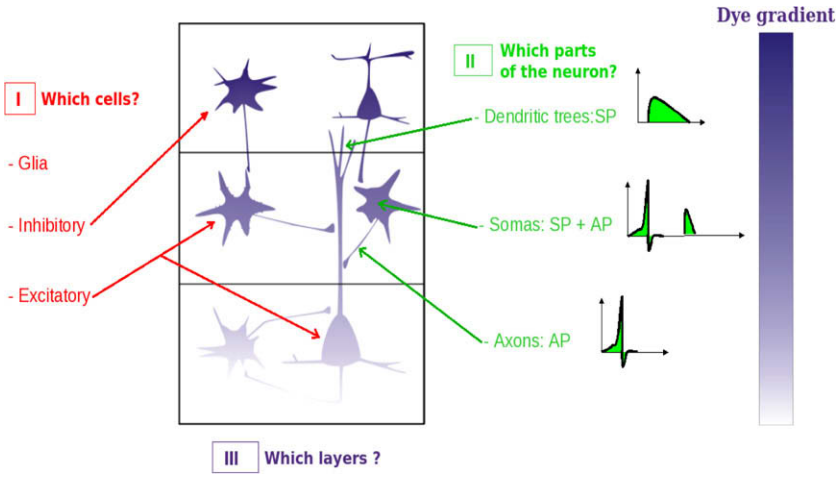

Fig. 2. Contributions of the optical signal. Once neurons are stained by the VSD, every neuronal membrane contributes to the resulting fluorescent signal, but from where? and in which proportion? Answering these four questions could clarify the optical signal origins: (1) Which cells? (2) Which parts of the cell? (3) Which layers? (4) Which presynaptic origins?

and it is more correct to state that the optical signal is multi-component since the VSD signal reflects the summed intracellular membrane potential changes of all neuronal compartments at a given cortical site. The aim then, is to determine the exact contribution of each component, which remains unknown. More precisely, what is quantitatively the contribution of dendritic activity? Can spiking activity be neglected?

3.4. About the contribution from cortical layers

The depth of the neocortex is about 2 mm. It is made up of six horizontal layers principally segregated by cell types and neuronal connections. The layer II mostly contains small pyramidal neurons that make strong connections with large pyramidal neurons of the layer V (Thomson and Morris, 2002).

Improved dyes, when put at the surface of the exposed cortex, can reach a depth of about 400–800 μm from the cortical surface, which mainly corresponds to superficial layers (Grinvald et al., 1999; Petersen et al., 2003). Furthermore, measures of the distribution of dye fluorescence intensity in rat visual and barrel cortex confirm that the optical signal mostly originates from superficial layers I–III (Ferezou et al., 2006; Lippert et al., 2007). Note that Lippert et al. (2007) used a special staining procedure, i.e. keeping the dura mater intact, but dried.

However, they did not take into account the fact that the activity in superficial layers could arise from neurons in deep layers, due to their dendritic arborization. Indeed, large pyramidal neurons in layer V have apical dendrites that reach superficial layers and may contribute to the signal. Therefore, the exact contribution of each cortical layer still has to be clarified.

3.5. About the contribution from thalamic versus horizontal connections

The origin of the signal can also be problematic when looking at the contribution from the different presynaptic activity origins, e.g. direct thalamic synaptic inputs, or horizontal inputs. Indeed, in response to a local stimulation, slow propagating waves can be recorded (Grinvald et al., 1994; Jancke et al., 2004; Roland et al., 2006; Xu et al., 2007; Benucci et al., 2007). We can question what is the relative contribution of all the synaptic input sources of this phenomenon, i.e. feedforward, horizontal or feedback inputs. Dedicated models could help teazing apart those various contributions.

3.6. Conclusion

Fig. 2 summarizes the four main questions not completely clarified to date:

(a) What are the contributions of the various neurons and neuronal components to the optical signal?
(b) What is the ratio between spiking and synaptic activity?
(c) What are the respective contributions of cells from deep versus superficial layers?
(d) What is the origin of the synaptic input? More precisely, what are the respective contributions of thalamic, local and long-range inputs?

To answer these questions, a possibility is to develop computational models in order to reproduce and analyse VSD signals. Models of VSD signals are reported in the next and last part of this review.

4. Benefits of modeling for optical signal analysis

The goal of this section is to investigate the different models from the literature, used to reproduce and analyse the VSD signal. We quickly emphasize three of these models because of their scale of analysis. In the last subsection, we present, in detail, an intermediate model that would allow to answer the previous questions about the VSD signal contributions.

4.1. Which scale for which model?

As previously described, the origin of the VSD signal is complex and remains to be estimated and explored. Therefore, it could be interesting to see if the activity of a computational model could be related to this signal. However, the choice of the model's scale is very important and depends on what exactly the model is designed for. We propose in the following paragraphs that the mesoscopic scale seems would be the best scale for analyzing the population VSD signal. In neuroscience, this scale is generally used to define the elementary processing unit in the brain, the cortical column. We start by defining our concept of cortical columns.

Since the 1950s, thanks to the work of Mountcastle (1957), we know that the cerebral cortex has a columnar organization. In 1960s and 1970s, Hubel and Wiesel (1962, 1965, 1977) followed

Please cite this article in press as: Chemla, S., Chavane, F. Voltage-sensitive dye imaging: Technique review and models. J. Physiol. (2009), doi:10.1016/j.jphysparis.2009.11.009

Mountcastle's discoveries by showing that ocular dominance and orientations are organized in a columnar manner in cat and monkey visual cortex. Today, the notion of cortical column becomes a large controversy since the original concept is expanding, year after year, discovery after discovery, to embrace a variety of different structures, principles and names. A 'column' now refers to cells in any vertical cluster that share the same tuning for any given receptive field attribute (see Horton and Adams (2005) for a detailed review on the cortical column concept). A novel and useful concept is to propose that each definition of cortical column depends on its type (anatomical, functional, physico-functional) and its spatial scale, as detailed in Table 2. A minicolumn or a microcolumn is an anatomical column of about 100 neurons, since its spatial scale is about 40 μm. Next, orientation or ocular dominance columns are classified as functional columns whose the spatial scale is between 200 and 300 μm, containing several minicolumns. An hypercolumn in V1 or a macrocolumn in the general case, then represents a physico-functional unit containing a full set of values for any given functional parameter. Its spatial scale can be up to 600 μm and contains about 10^4 neurons. Finally, neural mass is a mesoscopic concept which depends on the spatial scale. When looking at a cortical area, it can be used to represent, for example, all the pyramidal neurons contained in it (about 10^5 neurons).

Into these definitions and in order to reproduce exactly the same signal, i.e. time course and spatial extent, it seems appropriate to construct models at a large mesoscopic scale which could represent an entire cortical area. Models from Miikkulainen et al. (2005), Grimbert et al. (2007), Rangan et al. (2005) and La Rota (2003) consider this scale, that can be view as the neurons population scale.

An other point of view is to choose a much finer scale allowing to construct a more detailed biophysical model in order to quantitatively estimate the exact contribution of the VSD signal (excitation vs. inhibition, parts of the neuron, layers participation, etc.). In optical imaging, the visual scale studied, which is about 50 μm, corresponds to one pixel. It is still a population activity since it represents about 200 neurons, but the scale being relatively small, we will call it "intermediate mesoscopic scale". This model is detailed in the last section.

4.2. Mesoscopic scale: models of a cortical area

4.2.1. Extended LISSOM model

The Laterally Interconnected Synergetically Self-Organizing Map (LISSOM) family of models was developed by Bednar, Choe, Miikkulainen and Sirosh, at the University of Texas (Miikkulainen et al., 2005; Sirosh and Miikkulainen, 1994), as models of human visual cortex at a neural column level. It is based on the Self-Organizing Maps (SOM) algorithm (from Kohonen, 2001) used to visualize and interpret large high-dimensional data sets. When extended, the LISSOM neural network models takes into account lateral interactions (excitatory and inhibitory connections), allowing to reproduce the pinwheel organization of the primary visual cortex map, such as orientation, motion direction selectivity and ocular-dominance maps.

Sit and Miikkulainen used such a LISSOM model to represent V1 and tried to show how the activity of such a computational model of V1 can be related to the VSD signal (Sit and Miikkulainen, 2007). Indeed, with an extended LISSOM model including propagation delays in the cortical connections, they showed that the orientation tuning curve and the response dynamics of the model were similar to those measured with VSDI.

The model is a couple of two layers of neural units that represent the retina and V1. In V1, neural units account for a whole vertical column of cells. They receive input from the retina and also from neighbour columns (short-rang lateral excitatory and long-rang lateral inhibitory connections). Thus, the neuronal activity of unit $\mathbf{r}$ in V1 writes:

$$\begin{aligned} A(\mathbf{r},t) &= \sigma(V(\mathbf{r},t)),\\ V(\mathbf{r},t) &= \sum_{\rho}\gamma_{\rho}\sum_{\mathbf{r}'}W_{\rho,\mathbf{r},\mathbf{r}'}A(\mathbf{r}',t-d(\mathbf{r},\mathbf{r}'))+\sum_{\mathbf{s}}\chi_{\mathbf{s}}R_{\mathbf{s},\mathbf{r}}, \end{aligned} \quad (1)$$

where σ is a sigmoid activation function and the two terms are respectively the weighted sum of the lateral activations and the input activation from the retina. $W_{\rho,\mathbf{r},\mathbf{r}'}$ and $R_{\mathbf{s},\mathbf{r}}$ are respectively the synaptic weights matrix of lateral and retinal connections, and $d(\mathbf{r},\mathbf{r}')$ is the delay function between unit $\mathbf{r}$ and unit $\mathbf{r}'$. This is thus a scalar model of the neural activity.

Then, the computation of the VSD signal is done by looking only at the subthreshold activity $V(\mathbf{r},t)$, given by the weighted sum of presynaptic activity. To simplify, the authors have extended the LISSOM model with delayed lateral connections to compute the VSD signal from subthreshold signal. This is thus a scalar linear model of the VSD signal built on convolutions.

This model, based on Hebbian self-organizing mechanisms, is simple and efficient to replicate the detailed development of the primary visual cortex. It is thus very useful to study VSDI functional maps. However, this model is not specific enough to answer the previous asked questions (see Section 3.6).

4.2.2. Neural field model of a cortical area

Another approach, introduced by Grimbert et al. (2007) and Grimbert et al. (2008), proposes neural fields as a suitable mesoscopic models of cortical areas, in link with VSD. Neural field are continuous networks of interacting neural masses, describing the dynamics of the cortical tissue at the population level (Wilson and Cowan, 1972; Wilson et al., 1973). It could thus be applied to solve the direct problem of the VSD signal, providing the right parameters. More precisely, the authors showed that neural fields can easily integrate the biological knowledge of cortical structure, especially horizontal and vertical connectivity patterns. Hence, they proposed a biophysical formula to compute the VSD signal in terms of the activity of a field.

The classical neural field model equation is used, either written in terms of membrane potential or in terms of activity of the different neural masses present in a cortical column. For example, if $\mathbf{r}$ represents one spatial position of the spatial domain defining the area, then the underlying cortical column is described, at time t, by either a vector $\mathbf{V}(\mathbf{r},t)$ or $\mathbf{A}(\mathbf{r},t)$:

Table 2
The different types of cortical columns.

	Anatomical	Ol pixel	Functional	Physico-functional	Cortical area
Type of cortical column	Microcolumn or minicolumn	*Our column*	Orientation, ocular dominance column	Macrocolumn or hypercolumn (V1)	Neural mass
Spatial scale	40–50 μm	50–100 μm	200–300 μm	600 μm (and more)	10 mm
Number of neurons	80–100 neurons	200 neurons	Several minicolumns	60–100 minicolumns or 10,000 neurons	100X Thousand neurons of the same type (pyr, stellate, etc.)

Please cite this article in press as: Chemla, S., Chavane, F. Voltage-sensitive dye imaging: Technique review and models. J. Physiol. (2009), doi:10.1016/j.jphysparis.2009.11.009

$$\dot{\mathbf{V}}(\mathbf{r},t) = -\mathbf{L}\mathbf{V}(\mathbf{r},t) + \int_{\Omega} \mathbf{W}(\mathbf{r},\mathbf{r}')\mathbf{S}(\mathbf{V}(\mathbf{r}',t))d\mathbf{r}' + \mathbf{I}_{ext}(\mathbf{r},t), \quad (2)$$

and

$$\dot{\mathbf{A}}(\mathbf{r},t) = -\mathbf{L}\mathbf{A}(\mathbf{r},t) + \mathbf{S}\left(\int_{\Omega} \mathbf{W}(\mathbf{r},\mathbf{r}')\mathbf{A}(\mathbf{r}',t)d\mathbf{r}' + \mathbf{I}_{ext}(\mathbf{r},t)\right) \quad (3)$$

Here, $\mathbf{V}(\mathbf{r},t)$ contains the average soma membrane potentials of the different neural masses present in the column (the vector's dimension then represents the number of neuronal types considered in every column). $\mathbf{A}(\mathbf{r},t)$ contains the average activities of the masses. For example, A_i is the potential quantity of post-synaptic potential induced by mass i on the dendrites of all its post-synaptic partners. The actual quantity depends on the strength and sign (excitatory or inhibitory) of the projections (see Grimbert et al. (2007, 2008) and Faugeras et al. (2008) for more details on the model's equations). The model include horizontal intercolumnar connections and also vertical intracolumnar connections between neural masses. The latter gives an advantage to this model compared to the previous one, since the vertical connectivity was not taken into account in the extended LISSOM model. Furthermore, extracortical connectivity is not made explicit here, though taken into account in Grimbert et al. (2007).

Hence, based on this biophysical formalism (and especially the activity-based model), which is more adapted than the voltage-based model), the authors propose a formula involving the variables and parameters of a neural field model to compute the VSD signal:

$$OI(\mathbf{r},t) = \sum_{j=1}^{N} \int_{\Omega} \tilde{w}_j(\mathbf{r},\mathbf{r}')A_j(\mathbf{r}',t)d\mathbf{r}', \quad (4)$$

where $\tilde{w}_j(\mathbf{r},\mathbf{r}')$ contains all the biophysical parameters accounting for a cortical area structure stained by a voltage-sensitive dye, i.e. the different layers, the number of neurons, the number of dye molecules per membrane surface unit, the attenuation coefficient of light and also the horizontal and vertical distribution patterns of intra and intercortical connectivities.

This formula is the result of many decompositions of the total optical signal, from layer level to cellular membrane level, where the signal is simply proportional to the membrane potential.

Better than the Lissom model for our considerations, this large-scale model reproduces the spatiotemporal interactions of a cortical area in response to complex stimuli, e.g. line motion illusion, and allows, on average, to answer at the mesoscopic scale some previous questions (see Section 3.6). However, improvements on parameters tuning are still needed.

4.2.3. Conductance-based IAF neuronal network model

Another large-scale computational model of the primary visual cortex have been proposed by Rangan et al. (2005). The model is a two-dimensional patch of cortex, containing about 10^6 neurons with a preferred orientation, whose 80% are excitatory and 20% are inhibitory. The dynamics of single cell i is described by a single compartment, conductance-based, exponential integrate-and-fire equation (see Geisler et al. (2005) for more details on this neuron model). The derivation of this equation gives the membrane potential of neuron i of spatial position $\mathbf{r}_i$:

$$V(\mathbf{r}_i,t) = \frac{g^L V^L + (g_i^A(t) + g_i^N(t))V^E + g_i^G(t)V^I}{g^L + g_i^A(t) + g_i^N(t) + g_i^G(t)} \quad (5)$$

where g^L, g_i^A, g_i^N and g_i^G are respectively leak, AMPA, NMDA and GABA conductances, and V^L, V^E and V^I are respectively leak, excitatory and inhibitory reversal potentials.

The authors then use $V(\mathbf{r},t)$ to represent the VSD signal, i.e. the subthreshold dendritic activity in the superficial layers of the cortex. Poisson processes are used to simulate inputs from the thalamus and background noise.

This model allows, like the previous one Grimbert et al. (2007), to reproduce the spatiotemporal activity patterns of V1, as revealed by VSDI, in response to complex stimuli, e.g. the line motion illusion. However, in comparison with Grimbert et al. (2007), no laminar structure is taken into account.

4.2.4. Linear model of the raw VSD signal

With the same scale of analysis, La Rota (2003) presented an interesting linear model in order to study the neural sources of the mesoscopic VSD signal. The author chose a compromise between a detailed and a "black-box" model of the signal, by taking into account the important properties of the VSD signal and also the artefacts directly linked to its measure, in a mesoscopic, linear and additive model. The VSD signal of a cortical area can then be modeled by an intrinsic and an extrinsic components:

$$OI(t) = A(t) + \rho(t), \quad (6)$$

where $A(t)$ represents the activity of the intrinsic component of the optical signal (i.e. the synaptic activity of the cortical area observed) and $\rho(t)$ represents all the noise and artefacts due to the measure (e.g. hemodynamic artefact, cardiovascular and respiratory movements, instrumental noise, etc.). In this model, inputs from the thalamus are considered as background noise and thus enter in the ρ component.

The model is interesting because it both takes into account the intrinsic and the extrinsic variability of the VSD signal. The latter being supposed already removed, when analyzing the signal in the three other presented models.

4.3. Biophysical model at the intermediate mesoscopic scale

Since none of the previous models was specific enough to determine the different contributions of the optical signal, a biological cortical column model, at an intermediate mesoscopic scale, has also been proposed in order to better understand and interpret biological sources of VSD signals (Chemla et al., 2007). This scale corresponds to one pixel of optical imaging: about 50 μm and the related model solves the direct VSD problem, i.e. generates a VSD signal, given the neural substrate parameters and activities. Using a detailed compartmental model allows to push the state of the art at this level. This model confirms and quantifies the fact that the VSD signal is the result of an average from multiple components.

4.3.1. Model specifications

Into the above cortical columns paradigm and for our specific model, we introduced a new distinction of a cortical column (see Fig. 2, second column). The spatial scale is about 50 μm, corresponding to one pixel of optical imaging. Given this spatial scale, the number of neurons, that has been evaluated from Binzegger et al. (2004), is about 200.

We then consider a class of models based on a cortical microcircuit (see Raizada and Grossberg (2003), Douglas and Martin (2004), and Haeusler et al. (2007) for more details on this concept), whose synaptic connections are made only between six specific populations of neurons: two populations (excitatory and inhibitory) for three main layers (2/3, 4, 5/6).

Each neuron is represented by a reduced compartmental description (see Bush and Sejnowski (1993) for more details on the reduction method) with conductance-based Hodgkin–Huxley neuron model (see Hodgkin and Huxley, 1952) in the soma and the axon. Thus, the dynamics of single cells are described by the following equation:

Please cite this article in press as: Chemla, S., Chavane, F. Voltage-sensitive dye imaging: Technique review and models. J. Physiol. (2009), doi:10.1016/j.jphysparis.2009.11.009

$$C_m \frac{dV}{dt} = I_{ext} - \sum_i g^i(V)(V - V^i) \quad (7)$$

where V is the membrane potential, I_{ext} is an external current injected into the neuron, C_m is the membrane capacitance, and where three types of current are represented: leak, potassium and sodium conductances or respectively G_L, G_K and $G_N a$. G_L is independent of V and determines the passive properties of the cells near resting potential. The sodium and potassium conductances are responsible for the spike generation. Furthermore, a slow potassium conductance was included in the dynamics of the excitatory population to reproduce the observed adaptation of the spike trains emitted by these neurons (see Nowak et al., 2003). This feature seems to be absent in inhibitory neurons, as taken into account in this model.

Only passive dendrites were considered. Each neuron represented with seven to nine compartments. The link between compartments can then be described by Eq. (8) (Hines and Carnevale, 1997).

$$C_j \frac{dV_j}{dt} + Iion_j = \sum_k \frac{V_k - V_j}{R_j k} \quad (8)$$

where V_j is the membrane potential in compartment j, $Iion_j$ is the net transmembrane ionic current in compartment j, C_j is the membrane capacitance of compartment j and R_{jk} is the axial resistance between the centers of compartment j and adjacent compartment k.

Synaptic inputs are modeled as conductance changes. Excitatory AMPA synapses are converging on soma and dendrites of each neuron, whereas inhibitory GABA synapses are only converging on soma of each neuron (Salin and Bullier, 1995). The number of synapses involved in the projections between these different neuronal types, including the afferent from the LGN, were recalculated for a 50 μm cortical column, based on Binzegger et al. (2004) for the considered layers, while latencies have been introduced for each connection following Thomson et al. (2007).

Input signals from the thalamus into the neocortex layer IV was simulated by applying random spike trains to each neuron in layer IV and random latency have been introduced for each input connection to simulate the temporal properties of geniculocortical pathway. Then we increased the frequency of the spike trains in order to represent stimulus contrast and see how the model transforms an increasing input, i.e. the contrast response function (see Albrecht et al., 1982). At this point, the column is isolated. A step further, the conditions relative to a larger network are reproduced as follows: First, "background noise" was introduced in each neuron of the column. Typically, noise can be introduced in the form of stochastic fluctuation of a current or an ionic conductance. The stochastic model of Destexhe et al. (2001), containing two fluctuating conductances, is used here, allowing us to simulate synaptic background activity similar to in vivo measurements, for a large network. Second, lateral connections between two neighboring columns are reproduced by introducing an other set of random spike trains inputs whose frequency, synaptic delays and synaptic weights are adapted for fitting experimental data. Fig. 3 shows a schematic of the model, with thalamic input, background activity and lateral interactions. Examples of neuronal response have been plotted in function of increasing input or contrast.

4.3.2. Computation of the VSD signal

The VSD signal is simulated using a linear integration on the membrane surface of neuronal components. Here, the use of compartmental model has a real interest. Indeed, the computation of the VSD signal, for a given layer L, is given by:

$$OI^L = \lambda^L \sum_{i \in \{Compartments\}} V_i S_i \quad (9)$$

where S_i and V_i are respectively the surface and the membrane potential of the ith compartment and λ^L represents the fluorescence's gradient or the illumination intensity of the dye in layer L.

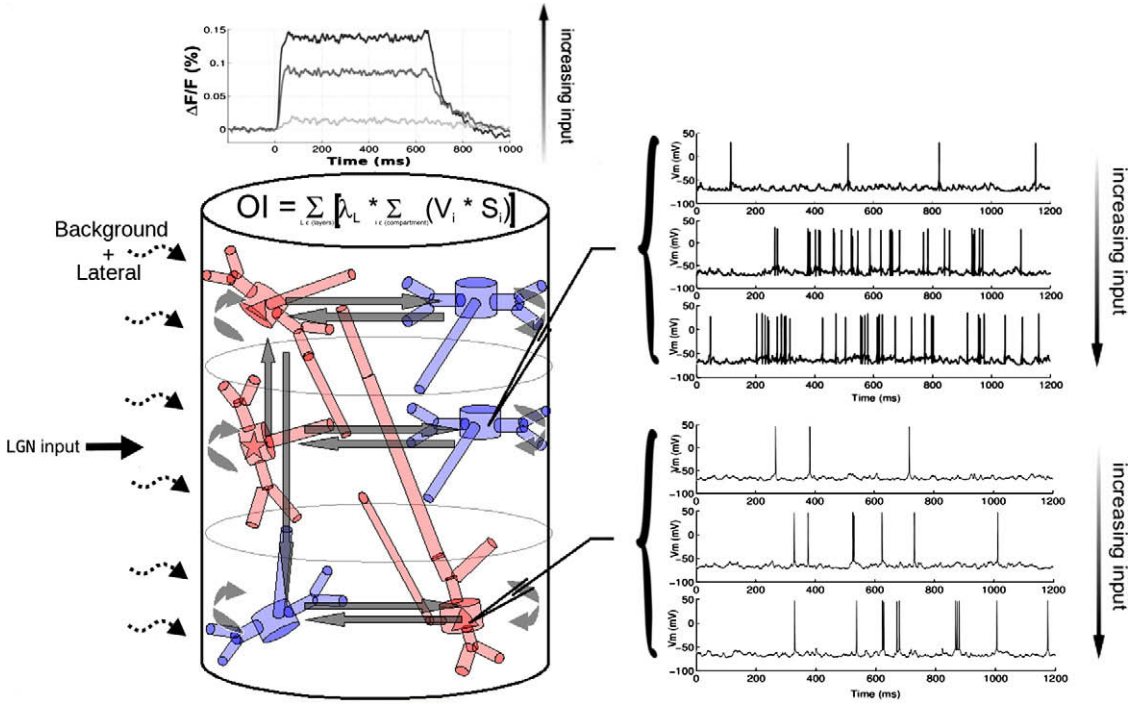

Fig. 3. Model representation taking into account thalamic input contrast, background activity and lateral connections and offering the possibility to compute the VSD signal with a linear formula. In output, inhibitory and excitatory neuronal responses are plotted in function of increasing input or contrast (right inset). The temporal evolution of the VSD signal in response to 600 ms stimuli and in function of increasing input is also emphasized.

Please cite this article in press as: Chemla, S., Chavane, F. Voltage-sensitive dye imaging: Technique review and models. J. Physiol. (2009), doi:10.1016/j.jphysparis.2009.11.009

Thus, this model takes into account soma, axon and dendrites influences, introduces 3D geometrical properties (dendrites of large pyramidal neurons in layer 5 can reach superficial layers) and fluorescence gradient depending on depth. According to Lippert et al. (2007) and Petersen et al. (2003), $\lambda^2 = 0.95$, $\lambda^4 = 0.05$ and $\lambda^5 = 0$. Then, the total optical imaging signal is given by the following formula:

$$OI = \sum_{L \in \{Layers\}} OI^L \tag{10}$$

Following this framework, the VSD signal is simulated in response to known stimuli (Fig. 3, bottom right inset) and compared to experimental results (Chemla et al., 2008).

Thanks to its compartmental construction, this model can predict the different contributions of the VSD signal. It thus gives the possibility to quantitatively answer the previous asked questions: excitation vs. inhibition, spiking vs. synaptic activity and superficial vs. deep layers: The model confirms that the VSD signal mainly reflects dendritic activity (75%) of excitatory neurons (80%) in superficial layers (80%). However, these numbers are changing when increasing the level of input activity. At high level of activity, inhibitory cells, spiking activity and deep layers become non-negligible, and should be taken into account in the computation of the VSD signal. These results will be the subject of a future publication.

5. Conclusion

In this review, we have presented the voltage-sensitive dyes imaging (VSDI) technique in a general and elementary manner. This optical technique, thanks to its excellent spatial and temporal resolution, offers many possibilities for *in vitro* and more interestingly *in vivo* brain imaging.

However, the recorded optical signal is multi-component and its origins are still unresolved. Indeed, the contribution of each component, i.e. glial cells, excitatory cells, inhibitory cells, somas, axons, dendrites, layers, is very difficult to isolate from the others.

This review suggests modeling as the appropriate solution. We reported four existing models that try to reproduce and analyse the VSD signal. The main advantage of these models, all built at a mesoscopic scale, is the ability to compare the same signal, i.e. the signal of an entire cortical area. However, for our considerations, i.e. find the different contributions of the VSD signal, those models have not the right scale. Thus, we proposed a biophysical cortical column model, at an intermediate mesoscopic scale, in order to find the biological sources of the VSD signal. Using a such compartmental model should be of great value for doing a quantitative analysis of the different contributions of the optical signal.

Acknowledgements

The authors are grateful to Thierry Vieville, from the CORTEX Lab., INRIA, Sophia-Antipolis, for his active participation in the model development and his help in writing this review. They also thank Francois Grimbert, at Northwestern University in the Department of Neurobiology and Physiology, for helpful discussions on the subject. Partially supported by the EC IP Project FP6015879, FACETS and the MACCAC ARC projects.

References

Ahmed, B., Hanazawa, A., Undeman, C., Eriksson, D., Valentiniene, S., Roland, P.E., 2008. Cortical dynamics subserving visual apparent motion. Cereb. Cortex 18 (12), 2796–2810.

Aitken, J.T., 1955. Observations on the larger anterior horn cells in the lumbar region of the cat's spinal cord. J. Anat. 89, 571.

Albowitz, B., Kuhnt, U., 1993. The contribution of intracortical connections to horizontal spread of activity in the neocortex as revealed by voltage sensitive dyes and a fast optical recording method. Eur. J. Neurosci. 5 (10), 1349–1359.

Albrecht, D., Hamilton, D., 1982. Striate cortex of monkey and cat: contrast response function. J. Neurophysiol. 48 (1), 217–233.

Antic, S., Zecevic, D., 1995. Optical signals from neurons with internally applied voltage-sensitive dyes. J. Neurosci. 15 (2), 1392–1405.

Antic, S., Major, G., Zecevic, D., 1999. Fast optical recordings of membrane potential changes from dendrites of pyramidal neurons. J. Neurophysiol. 82 (3), 1615–1621.

Arieli, A., Shoham, D., Hildesheim, R., Grinvald, A., 1995. Coherent spatiotemporal patterns of ongoing activity revealed by real-time optical imaging coupled with single-unit recording in the cat visual cortex. J. Neurophysiol. 73 (5), 2072–2093.

Arieli, A., Sterkin, A., Grinvald, A., Aerster, A., 1996. Dynamics of ongoing activity: explanation of the large variability in evoked cortical responses. Science 273 (5283), 1868–1871.

Benucci, A., Robert, A.F., Carandini, M., 2007. Standing waves and traveling waves distinguish two circuits in visual cortex. Neuron 55 (1), 103–117.

Berger, T., Borgdorff, A., Crochet, S., Neubauer, F.B., Lefort, S., Fauvet, B., Ferezou, I., Carleton, A., Luscher, H.R., Petersen, C.C., 2007. Combined voltage and calcium epifluorescence imaging in vitro and in vivo reveals subthreshold and suprathreshold dynamics of mouse barrel cortex. J. Neurophysiol. 97 (5), 3751–3762.

Binzegger, T., Douglas, R., Martin, K., 2004. A quantitative map of the circuit of cat primary visual cortex. J. Neurosci. 24 (39), 8441–8453.

Blasdel, G.G., Salama, G., 1986. Voltage-sensitive dyes reveal a modular organization in monkey striate cortex. Nature 321 (6070), 579–585.

Bolz, J., Novak, N., Staiger, V., 1992. Formation of specific afferent connections in organotypic slice cultures from rat visual cortex cocultured with lateral geniculate nucleus. J. Neurosci. 12 (8), 3054–3070.

Bonhoeffer, T., Grinvald, A., 1991. Iso-orientation domains in cat visual cortex are arranged in pinwheel-like patterns. Nature 353 (6343), 429–431.

Borg-Graham, L., Monier, C., Fregnac, Y., 1998. Visual input evokes transient and strong shunting inhibition in visual cortical neurons. Nature 393, 369–373.

Brown, C.E., Aminoltejari, K., Erb, H., Winship, I.R., Murphy, T.H., 2009. In vivo voltage-sensitive dye imaging in adult mice reveals that somatosensory maps lost to stroke are replaced over weeks by new structural and functional circuits with prolonged modes of activation within both the peri-infarct zone and distant sites. J. Neurosci. 29 (6), 1719–1734.

Bush, P., Sejnowski, T., 1993. Reduced compartmental models of neocortical pyramidal cells. J. Neurosci. Methods 46, 159–166.

Cameron, R.S., Rakic, P., 1991. Glial cell lineage in the cerebral cortex: a review and synthesis. Glia 4, 124–137.

Carlson, G.C., Coulter, D.A., 2008. In vitro functional imaging in brain slices using fast voltage-sensitive dye imaging combined with whole-cell patch recording. Nat. Protocols 3 (2), 249–255.

Chemla, S., Chavane, F., Vieville, T., Kornprobst, P., 2007. Biophysical cortical column model for optical signal analysis. In: Cns07. <http://www.cnsorg.org>.

Chemla, S., Vieville, T., Chavane, F., 2008. Biophysical cortical column model for optical signal analysis. In: Areadne08. <http://www.areadne.org/>.

Cinelli, A.R., Salzberg, B.M., 1990. Multiple site optical recording of transmembrane voltage (msortv), single-unit recordings, and evoked field potentials from the olfactory bulb of skate (raja erinacea). J. Neurophysiol. 64 (6), 1767–1790.

Cinelli, A.R., Salzberg, B.M., 1992. Dendritic origin of late events in optical recordings from salamander olfactory bulb. J. Neurophysiol. 68 (3), 786–806.

Civillico, E.F., Contreras, D., 2006. Integration of evoked responses in supragranular cortex studied with optical recordings in vivo. J. Membr. Biol. 96 (1), 336–351.

Cohen, L., Salzberg, B.M., Davila, H.V., Ross, W.N., Landowne, D., Waggoner, A.S., Wang, C.H., 1974. Changes in axon fluorescence during activity: molecular probes of membrane potential. J. Membr. Biol. 19 (1), 1–36.

Contreras, D., Llinas, R., 2001. Voltage-sensitive dye imaging of neocortical spatiotemporal dynamics to afferent activation frequency. J. Neurosci. 21 (23), 9403–9413.

Davila, H.V., Salzberg, B.M., Cohen, L.B., Waggoner, A.S., 1973. A large change in axon fluorescence that provides a promising method for measuring membrane potential. Nat. New Biol. 241 (109), 159–160.

Derdikman, D., Hildesheim, R., Ahissar, E., Arieli, A., Grinvald, A., 2003. Imaging spatiotemporal dynamics of surround inhibition in the barrels somatosensory cortex. J. Neurosci. 23 (8), 3100–3105.

Destexhe, A., Rudolph, M., Fellous, J., Sejnowski, T., 2001. Fluctuating synaptic conductances recreate in-vivo-like activity in neocortical neurons. Neuroscience 107, 13–24.

Douglas, R.J., Martin, K.A.C., 1990. Neocortex. In: shepeherd, G. (Ed.), Synaptic Organization of the Brain. Oxford University Press, New York, pp. 220–248.

Douglas, R., Martin, K.A.C., 2004. Neuronal circuit of the neocortex. Ann. Rev. Neurosci. 27, 419.

Eberwine, J., 2001. Molecular biological of axons: a turning point. Neuron 32 (6), 959–960.

Ebner, T.J., Chen, G., 1995. Use of voltage-sensitive dyes and optical recordings in the central nervous system. Prog. Neurobiol. 46 (5), 463–506.

Faugeras, O., Grimbert, F., Slotine, J.-J., 2008. Absolute stability and complete synchronization in a class of neural fields models. SIAM J. Appl. Math. 61 (1), 205–250.

Ferezou, I., Bolea, S., Petersen, C.C.H., 2006. Visualizing the cortical representation of whisker touch: voltage-sensitive dye imaging in freely moving mice. Neuron 50, 617–629.

Please cite this article in press as: Chemla, S., Chavane, F. Voltage-sensitive dye imaging: Technique review and models. J. Physiol. (2009), doi:10.1016/j.jphysparis.2009.11.009

Geisler, C., Brunel, N., Wang, X.-J., 2005. Contributions of intrinsic membrane dynamics to fast network oscillations with irregular neuronal discharges. J. Neurophysiol. 94, 4344–4361.

Grimbert, F., Faugeras, O., Chavane, F., 2007. From neural fields to VSD optical imaging. In: Cns07. <http://www.cnsorg.org>.

Grimbert, F., Faugeras, O., Chavane, F., 2008. Neural field model of vsd optical imaging signals. In: Areadne08. <http://www.areadne.org/>.

Grinvald, A., Manker, A., Segal, M., 1982. Visualization of the spread of electrical activity in rat hippocampal slices by voltage-sensitive optical probes. J. Physiol. 333, 269–291.

Grinvald, A., Anglister, L., Freeman, J.A., Hildesheim, R., Manker, A., 1984. Real time optical imaging of naturally evoked electrical activity in the intact frog brain. Nature 308 (5962), 848–850.

Grinvald, A., Frostig, R.D., Siegel, R.M., Bartfeld, E., 1991. High-resolution optical imaging of functional brain architecture in the awake monkey. Proc. Natl. Acad. Sci. USA 88 (24), 11559–11563.

Grinvald, A., Lieke, E., Frostig, R.D., Hildesheim, R., 1994. Cortical point-spread function and long-range lateral interactions revealed by real-time optical imaging of macaque monkey primary visual cortex. J. Neurosci. 14, 2545–2568.

Grinvald, A., Shoham, D., Shmuel, A., Glaser, D., Vanzetta, I., Shtoyerman, E., Slovin, H., Arieli, A., 1999. In-vivo optical imaging of cortical architecture and dynamics. In: Windhorst, U., Johansson, H. (Eds.), Modern Techniques in Neuroscience Research. Springer Verlag, pp. 893–969.

Grinvald, A., Hildesheim, R., 2004. Vsdi: a new era in functional imaging of cortical dynamics. Nature 5, 874–885. <www.nature.com/reviews/neuro>.

Gupta, R.G., Salzberg, B.M., Grinvald, A., Cohen, L., Kamino, K., Boyle, M.B., Waggoner, S., Wang, C.H., 1981. Improvements in optical methods for measuring rapid changes in membrane potential. J. Membr. Biol. 58 (2), 123–137.

Haeusler, S., Maass, W., 2007. A statistical analysis of information-processing properties of lamina-specific cortical microcircuits models. Cereb. Cortex 17 (January), 149–162.

Hines, M., Carnevale, N., 1997. The neuron simulation environment. Neural Comput. 9, 1179–1209.

Hodgkin, A., Huxley, A., 1952. A quantitative description of membrane current and its application to conduction and excitation in nerve. J. Physiol. 117, 500–544.

Horton, J., Adams, D.L., 2005. The cortical column: a structure without a function. Philos. Trans. R. Soc. Lond. B. Biol. Sci. 360 (1456), 837–862.

Hubel, D., Wiesel, T., 1962. Receptive fields, binocular interaction and functional architecture in the cat visual cortex. J. Physiol. 160, 106–154.

Hubel, D., Wiesel, T., 1965. Receptive fields and functional architecture in two nonstriate visual areas (18 and 19) of the cat. J. Neurophysiol. 28, 229–289.

Hubel, D., Wiesel, T., 1977. Functional architecture of macaque monkey. Proc. Roy. Soc., Lond. [B], 1–59.

Hubener, M., Shoham, D., Grinvald, A., Bonhoeffer, T., 1997. Spatial relationships among three columnar systems in cat area 17. J. Neurosci. 17 (23), 9270–9284.

Jancke, D., Chavane, F., Naaman, S., Grinvald, A., 2004. Imaging cortical correlates of illusion in early visual cortex. Nature 428, 423–426.

Jin, W., Zhang, R., Wu, J., 2002. Voltage-sensitive dye imaging of population neuronal activity in cortical tissue. J. Neurosci. Methods 115, 13–27.

Kauer, J.S., 1988. Real-time imaging of evoked activity in local circuits of the salamander olfactory bulb. Nature 331 (6152), 166–168.

Kee, M.Z., Wuskell, J.P., Loew, L.M., Augustine, G.J., Sekino, Y., 2009. Imaging activity of neuronal populations with new long-wavelength voltage-sensitive dyes. Brain Cell Biol. 36 (5–6), 157–172.

Kelly, J.P., Van Essen, D.C., 1974. Cell structure and function in the visual cortex of the cat. J. Physiol. 238, 515–547.

Kohonen, T., 2001. Self-Organizing Maps, third extended ed. Springer.

Konnerth, A., Orkand, R.K., 1986. Voltage-sensitive dyes measure potential changes in axons and glia of the frog optic nerve. Neurosci. Lett. 66 (1), 49–54.

Konnerth, A., Obaid, A.L., Salzberg, B.M., 1987. Optical recording of electrical activity from parallel fibres and other cell types in skate cerebellar slices in vitro. J. Physiol. 393, 681–702.

Konnerth, A., Orkand, P.M., Orkand, R.K., 1988. Optical recording of electrical activity from axons and glia of frog optic nerve: potentiometric dye responses and morphometrics. Glia 1 (3), 225–232.

Kubota, M., Hosokawa, Y., Horikawa, J., 2006. Layer-specific short-term dynamics in network activity in the cerebral cortex. Neuroreport 17 (11), 1107–1110.

Laaris, N., Keller, A., 2002. Functional independence of layer iv barrels. J. Neurophysiol. 87 (2), 1028–1034.

La Rota, C., 2003. Analyse de l'activité électrique multi-ties du cortex auditif chez le cobaye. Ph.D. Thesis, Université Joseph Fourier, Grenoble I.

Lev-Ram, V., Grinvald, A., 1986. Ca^{2+}- and K^{+}-dependent communication between central nervous system myelinated axons and oligodendrocytes revealed by voltage-sensitive dyes. Proc. Natl. Acad. Sci. USA 83 (17), 6651–6655.

Lippert, M.T., Takagaki, K., Xu, W., Huang, X., Wu, J.Y., 2007. Methods for voltage-sensitive dye imaging of rat cortical activity with high signal-to-noise ratio. J. Neurophysiol. 98, 502–512.

Manis, P.B., Freeman, J.A., 1988. Fluorescence recordings of electrical activity in goldfish optic tectum in vitro. J. Neurosci. 8 (2), 383–394.

Miikkulainen, R., Bednar, J.A., Choe, Y., Sirosh, J., 2005. Computational Maps in the Visual Cortex. Springer, Berlin.

Mountcastle, V., 1957. Modality and topographic properties of single neurons of cat's somatosensory cortex. J. Neurophysiol. 20, 408–434.

Nelson, D.A., Katz, L.C., 1995. Emergence of functional circuits in ferret visual cortex visualized by optical imaging. Neuron 15 (1), 23–34.

Nowak, L.G., Azouz, R., Sanchez-Vives, M.V., Gray, C., McCormick, D., 2003. Electrophysiological classes of cat primary visual cortical neurons in vivo as revealed by quantitative analyses. J. Neurophysiol. 89, 1541–1566. <http://jn.physiology.org/cgi/content/abstract/89/3/1541>.

Orbach, H.S., Cohen, L.B., 1983. Optical monitoring of activity from many areas of the in vitro and in vivo salamander olfactory bulb: a new method for studying functional organization in the vertebrate central nervous system. J. Neurosci. 3, 2251–2262.

Orbach, H.S., Van Essen, D.C., 1993. In vivo tracing of pathways and spatio-temporal activity patterns in rat visual cortex using voltage sensitive dyes. Exp. Brain Res. 94 (3), 371–392.

Orbach, H.S., Cohen, L.B., Grinvald, A., 1985. Optical mapping of electrical activity in rat somatosensory and visual cortex. J. Neurosci. 5, 1886–1895.

Petersen, C., Sakmann, B., 2001. Functional independent columns of rat somatosensory barrel cortex revealed with voltage-sensitive dye imaging. J. Neurosci. 21 (21), 8435–8446.

Petersen, C., Grinvald, A., Sakmann, B., 2003. Spatiotemporal dynamics of sensory responses in layer 2/3 of rat barrel cortex measured in vivo by voltage-sensitive dye imaging combined with whole-cell voltage recordings and neuron reconstructions. J. Neurosci. 23 (3), 1298–1309.

Raizada, R., Grossberg, S., 2003. Towards a theory of the laminar architecture of the cerebral cortex: computational clues from the visual system. Cereb. Cortex 13, 100–113.

Rangan, A.V., Cai, D., McLaughlin, D.W., 2005. Modeling the spatiotemporal cortical activity associated with the line-motion illusion in primary visual cortex. Proc. Natl. Acad. Sci. USA 102 (52), 18793–18800.

Reynaud, A., Barthelemy, F., Masson, G., Chavane, F., 2007. Input–output transformation in the visuo-oculomotor network. Arch. Ital. Biol., 145.

Roland, P.E., 2002. Dynamic depolarization fields in the cerebral cortex. Trends Neurosci. 25.

Roland, P.E., Hanazawa, A., Undeman, C., Eriksson, D., Tompa, T., Nakamura, H., Valentiniene, S., Ahmed, B., 2006. Cortical feedback depolarization waves: a mechanism of top-down influence on early visual areas. Proc. Natl. Acad. Sci. USA 103 (33), 12586–12591.

Ross, W.N., Salzberg, B.M., Cohen, L.B., Grinvald, A., Davila, H.V., Waggoner, A.S., Wang, C.H., 1977. Changes in absorption, fluorescence, dichroism, and birefringence in stained giant axons: optical measurements of membrane potential. J. Membr. Biol. 33 (1–2), 141–183.

Rubin, B.D., Katz, L.C., 1999. Optical imaging of odorant representations in the mammalian olfactory bulb. Neuron 23 (3), 499–511.

Salin, P., Bullier, J., 1995. Corticocortical connections in the visual system: structure and function. Psychol. Bull. 75, 107–154.

Salzberg, B.M., Davila, H.V., Cohen, L.B., 1973. Optical recording of impulses in individual neurons of an invertebrate central nervous system. Nature 246, 508–509.

Schummers, J., Yu, H., Sur, M., 2008. Tuned responses of astrocytes and their influence on hemodynamic signals in the visual cortex. Science 320, 1638–1643.

Seidemann, E., Arieli, A., Grinvald, A., Slovin, H., 2002. Dynamics of depolarization and hyperpolarization in the frontal cortex and saccade goal. Science 295 (5556), 862–865.

Sharon, D., Grinvald, A., 2002. Dynamics and constancy in cortical spatiotemporal patterns of orientation processing. Science 295 (5554), 512–515.

Sharon, D., Jancke, D., Chavane, F., Na'aman, S., Grinvald, A., 2007. Cortical response field dynamics in cat visual cortex. Cereb. Cortex 17 (12), 2866–2877.

Shoham, D., Glaser, D., Arieli, A., Kenet, T., Wijnbergeb, C., Toledo, Y., Hildesheim, R., Grinvald, A., 1999. Imaging cortical dynamics at high spatial and temporal resolution with novel blue voltage-sensitive dyes. Neuron 24 (4), 791–802.

Sholl, D.A., 1955a. The organization of the visual cortex in the cat. J. Anat. 89, 33–46.

Sirosh, J., Miikkulainen, R., 1994. Cooperative self-organization of afferent and lateral connections in cortical maps. Biol. Cybern. 71, 66–78.

Sit, Y.F., Miikkulainen, R., 2007. A computational model of the signals in optical imaging with voltage-sensitive dyes. Neurocomputing 70 (10–12), 1853–1857.

Slovin, H., Arieli, A., Hildesheim, R., Grinvald, A., 2002. Long-term voltage-sensitive dye imaging reveals cortical dynamics in behaving monkeys. J. Neurophysiol. 88 (6), 3421–3438.

Spors, H., Grinvald, A., 2002. Spatio-temporal dynamics of odor representations in the mammalian olfactory bulb. Neuron 34 (2), 301–315.

Sterkin, A., Lampl, I., Ferster, D., Grinvald, A., Arieli, A., 1998. Realtime optical imaging in cat visual cortex exhibits high similarity to intracellular activity. Neurosci. Lett. 51.

Tasaki, I., Watanabe, A., Carnay, L., 1968. Changes in fluorescence, turbidity, and bireference associated with nerve excitation. Proc. Natl. Acad. Sci. USA 61, 883–888.

Thomson, A., Lamy, C., 2007. Functional maps of neocortical local circuitry. Front. Neurosci. 1 (1), 19–42.

Thomson, A., Morris, O., 2002. Selectivity in the inter-laminar connections made by neocortical neurones. J. Neurocytol. 31 (3–5), 239–246.

Ts'o, D.Y., Frostig, R.D., Lieke, E.E., Grinvald, A., 1990. functional organization of primate visual cortex revealed by high resolution optical imaging. Science 249 (4967), 417–420.

Tucker, T.R., Katz, L.C., 2003a. Recruitment of local inhibitory networks by horizontal connections in layer 2/3 of ferret visual cortex. J. Neurophysiol. 89 (1), 501–512.

Please cite this article in press as: Chemla, S., Chavane, F. Voltage-sensitive dye imaging: Technique review and models. J. Physiol. (2009), doi:10.1016/j.jphysparis.2009.11.009

Tucker, T.R., Katz, L.C., 2003b. Spatiotemporal patterns of excitation and inhibition evoked by the horizontal network in layer 2/3 of ferret visual cortex. J. Neurophysiol. 89 (1), 488–500.

Waggoner, A.S., Grinvald, A., 1977. Mechanisms of rapid optical changes of potential sensitive dyes. Ann. NY Acad. Sci. 30 (303), 217–241.

Waters, J., Schaefer, A., Sakmann, B., 2005. Backpropagating action potentials in neurones: measurement, mechanisms and potential functions. Prog. Biophys. Mol. Biol. 87 (1), 145–170.

Wilson, H., Cowan, J., 1972. Excitatory and inhibitory interactions in localized populations of model neurons. Biophys. J. 12, 1–24.

Wilson, H., Cowan, J., 1973. A mathematical theory of the functional dynamics of cortical and thalamic nervous tissue. Biol. Cybern. 13 (2), 55–80.

Woolum, J.C., Strumwasser, F., 1978. Membrane-potential-sensitive dyes for optical monitoring of activity in aplysia neurons. J. Neurobiol. 9 (3), 185–193.

Xu, W., Huang, X., Takgaki, K., Wu, J., 2007. Compression and reflection of visually evoked cortical waves. Neuron 55 (1), 119–129.

Yang, Z., Heeger, D.J., Seidemann, E., 2007. Rapid and precise retinotopic mapping of the visual cortex obtained by voltage-sensitive dye imaging in the behaving monkey. J. Neurophysiol. 98 (2), 1002–1014.

Young, J.Z., 1958. Anatomical considerations. EEG Clin. Neurophysiol. 10, 9–11.

Yuste, R., Tank, D.K., Kleinfeld, D., 1997. Functional study of the rat cortical microcircuitry with voltage-sensitive dye imaging of neocortical slices. Cereb. Cortex 7 (6), 546–558.

Zochowski, M., Wachowiak, M., Falk, C.X., Cohen, L.B., Lam, Y.W., Antic, S., Zecevic, D., 2000. Imaging membrane potential with voltage-sensitive dyes. Biol. Bull. 198 (1), 749–762.

Please cite this article in press as: Chemla, S., Chavane, F. Voltage-sensitive dye imaging: Technique review and models. J. Physiol. (2009), doi:10.1016/j.jphysparis.2009.11.009